Bioimaging **3** (1995) 108–120. Printed in the UK

Simulation of the distribution of chromosome targets in cell nuclei under topological constraints

Christian Münkel†‡, Roland Eils†§, Jorg Imhoff†‖, Steffen Dietzel¶, Christoph Cremer+§ and Thomas Cremer¶§*

† Graduate college 'Modeling and Scientific Computing in Mathematics and Science', IWR, University of Heidelberg, D-69120 Heidelberg, Germany
‡ German Cancer Research Center, Biophysics of Macromolecules, INFZ80, D-69120 Heidelberg, Germany
§ Interdisciplinary Center of Scientific Computing (IWR), University of Heidelberg, D-69120 Heidelberg, Germany
‖ Institute of Theoretical Physics, University of Heidelberg, D-69120 Heidelberg, Germany
¶ Institute of Human Genetics and Anthropology, University of Heidelberg, D-69120 Heidelberg, Germany
+ Institute of Applied Physics, University of Heidelberg, D-69120 Heidelberg, Germany

Submitted 29 December 1994, accepted 13 November 1995

Abstract. Several models for the distribution of subchromosomal targets under topological constraints were developed which take into account that chromosomes occupy distinct, mutually exclusive territories in the cell nucleus. Nuclei and two pairs of chromosome territories of various size were modeled by spheres or ellipsoids under the simplified assumption that the entire set of chromosome territories present in a diploid cell nucleus completely fills the nuclear interior and that each territory occupies a fraction of the nuclear volume proportional to its DNA content. Monte Carlo simulations of the distribution of the territory gravity centers were performed taking into account the constraint of territory extension by the nuclear boundary and the constraint of territory self avoidance, i.e. territories should not intersect each other. In addition, various assumptions were made with regard to the location of point-like targets either within or at the surface of two 'homologous' model territories. For each assumption the distance between the two point-like targets and between each target and the center of the model nucleus was calculated in Monte Carlo simulations and in part also analytically. The distribution of point-like targets in model nuclei under the influence of these topological constraints depends on the shape of the model nucleus and shows strong deviations from a model often applied in previous studies. In this model the random distribution of point-like targets was described under the assumption that such targets are distributed uniformly and independently from each other within the nuclear space without any constraints except for the nuclear boundary. All models were applied to experimentally measured distributions of chromosomal subregions delineated by fluorescence *in situ* hybridization with subregion specific probes. We demonstrate that a neglect of geometrical constraints in the simulation of target distributions can lead to erroneous conclusions of whether experimental target distributions occur in a random manner or not.

Keywords: nuclear architecture, topography of chromosome territories, Monte Carlo simulations

1. Introduction

In spite of rapid progress in the linear physical mapping of the human and other genomes, the three-dimensional

* To whom correspondence should be addressed at: Institut für Humangenetik und Anthropologie, Universität Heidelberg, Im Neuenheimer Feld 328, D-69120 Heidelberg, Germany

0966-9051/95/030108+13$19.50

organization and distribution of genetic material in the cell nucleus is still largely unknown. While it has been predicted already at the turn of this century that chromosomes occupy distinct territories in animal and plant cell nuclei, experimental evidence for this hypothesis was provided only recently (for review see Cremer *et al* 1993). Non-radioactive *in situ* hybridization procedures with chromosome specific composite and subregional DNA probes have made possible the visualization of entire individual chromosome territories together with subchromosomal targets, e.g. centromeric heterochromatin or individual genes, in cell nuclei of various animal and plant species (Schardin *et al* 1985, Manuelidis 1985, Lichter *et al* 1988, Manuelidis and Borden 1988, Pinkel *et al* 1988, van Dekken *et al* 1989, Heslop-Harrison 1990, Popp *et al* 1990, Geiger *et al* 1991, Höfers *et al* 1993, Carter *et al* 1993, Cremer *et al* 1993). These studies have suggested cell type specific differences in intranuclear chromosomal arrangements (for review see Manuelidis 1990). Recently, light microscopic axial tomography was applied to measure three-dimensional distances between hybridized chromosome targets (Dietzel *et al*, see accompanying paper).

In previous studies (Später 1975, Rappold *et al* 1984, Klar *et al* 1984, Emmerich *et al* 1989, Popp *et al* 1990, Höfers *et al* 1993), attempts to decide whether subchromosomal targets are distributed randomly or non-randomly within the cell nucleus were based on a comparison with model nuclei of similar shapes (represented by spheres, ellipsoids or flat cylinders) taking into account the uniform and independent distribution of point-like targets within the entire nuclear space. This approach, however, did not take into account geometrical restrictions of target distributions which result from the fact that subchromosomal targets are part of the much larger chromosome territories. Present evidence based on 3-D-reconstructions of laser confocal serial sections from entire, fluorescently labeled chromosome territories suggests that each chromosome territory occupies a nuclear subvolume which is largely exclusive from other, neighboring territories, i.e. intermingling of chromatin fibers from a given chromosome territory with chromatin fibers from a neighboring territory appears to be limited to the territory periphery (Eils *et al* 1996). Subchromosomal targets (e.g. individual genes, centromeric and (sub-)telomeric DNA sequences) colocalize with their respective chromosome territory (Eils *et al* 1995a,b, and our unpublished data).

In the present study we describe and test improved models which take into account the distribution of subchromosomal targets under geometrical constraints resulting from the size and shape of chromosome territories, their location in the territory interior or at its surface as well as from the shape of the cell nucleus. Analytical calculations and Monte Carlo simulations demonstrate that the distribution of point-like chromosomal targets strongly depends on these constraints. Thus the spatial extension of chromosome territories and nuclear shape must not be neglected if an experimental distribution is compared with theoretical probability distributions.

2. Models and Monte Carlo simulations

2.1. Geometrical models of the cell nucleus

For three-dimensional Monte Carlo simulations the cell nucleus and two pairs of chromosome territories were modeled by spheres or ellipsoids with arbitrary axis lengths. Subchromosomal targets were assumed to be point-like. In one case two-dimensional modeling was performed. In this case the nucleus and the two pairs of chromosome territories were modeled either by circles or by ellipses (see section 3.1.3). For Monte Carlo simulations of 3-D-arrangements of point-like targets (see section 2.2), five models were considered (figure 1).

- Model 1: uniform and independent distribution of targets within the nucleus.
- Model 2: distribution of the mass centers of chromosome territories.
- Model 3: random location of targets within the chromosome territory.
- Model 4: random location of targets at the surface of the chromosome territory.
- Model 5: targets representing ‘centromeres’ are located at the surface of the chromosome territories with an orientation towards a ‘centrosome’ (reflected by a point located at the surface of the modeled cell nucleus). This orientation is performed in such a way that the distance of the target to the ‘centrosome’ is minimized.

If the distribution of point-like targets was not affected by the fact that they are part of chromosome territories, model 1 would be an appropriate description of a random distribution. In models 2–5 we assumed (i) that chromosome territories fill the nuclear space entirely in a mutually exclusive way and (ii) that the space occupied by a given territory is directly proportional to its DNA content. In addition, models 2–5 take into account two important geometrical constraints. One constraint results from the fact that the nuclear boundary provides a limit to the outward extension of each territory, i.e. territories must not intersect the nuclear boundary (constraint of territory extension). The other constraint is given by the assumption that territories occupy mutually exclusive nuclear subvolumes and thus must not intersect each other (constraint of territory self-avoidance). Model 2 can be used to describe a ‘random’ distribution of the mass centers of entire chromosome territories under these two geometrical constraints. Model 3 is compatible with the description of the chromatin fiber as a random chain confined within a spherical territory (Hahnfeldt *et al* 1993, Sachs *et al* 1995). Alternatively, model 4 assumes that targets are specifically exposed at the territory

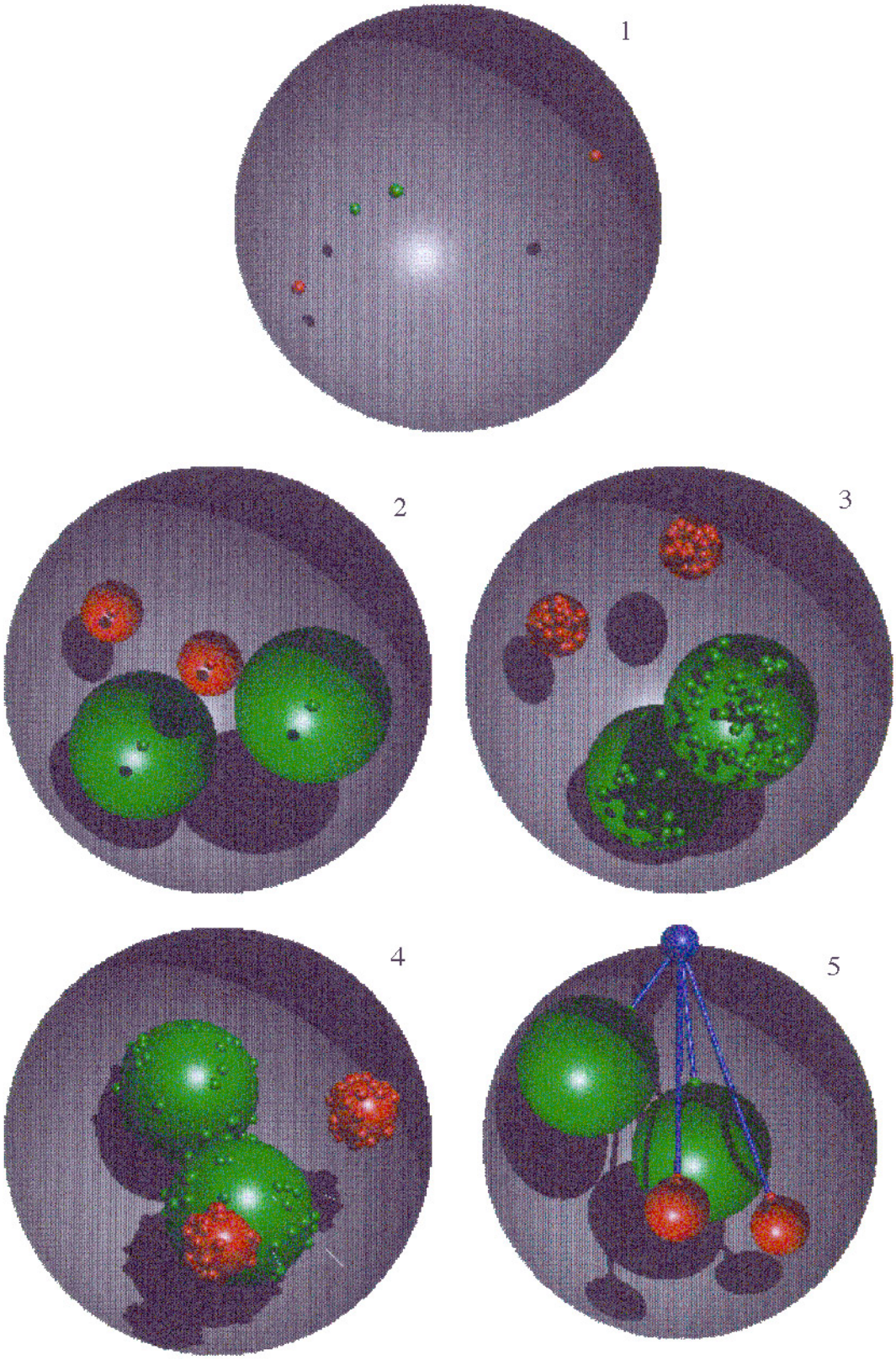

Figure 1. Illustrations of models 1–5 (for details see section 2.1).

surface owing to a specific three-dimensional folding of the chromatin fiber. Model 5 introduces an additional topological constraint of target positioning due to a specific orientation of chromosome territories in the cell nucleus, which in part reflects a 'Rabl-orientation', although we did not consider the assembly of all centromeres in a 'Rabl-Polfeld' (Rabl 1885, Cremer *et al* 1982). Applying models 2–5 we wished to determine to which extent target distributions under geometrical constraints would differ from model 1 and from each other.

2.2. Monte Carlo simulations

The three-dimensional distribution of chromosome territories or subchromosomal targets was calculated by Monte Carlo simulations (Binder and Heermann 1993, Kalos and Whitlock 1986). The following abbreviations are used:

R radius of spherically shaped nucleus or axis length of ellipsoidal nucleus
r radius of spherically shaped territory
r_S radius of smaller (subscript S) territory
r_L radius of larger (subscript L) territory

In each Monte Carlo simulation step the center of each territory was placed according to a uniform distribution and independently from other territories in a cube that circumscribed the model cell nucleus. In a first step whether the positions of territory centers fell within the model cell nucleus or outside was examined. In the latter case the configuration was rejected. Subsequently, an examination of whether a given territory, whose location was uniquely determined by the position of its center, intersected the surface of the model cell nucleus (violation of the constraint of territory extension) or whether two different territories intersected each other (violation of the constraint of territory self-avoidance) was carried out. When one or both constraints were violated, the respective configuration was rejected. Model targets were then placed either within or at the surface of the respective chromosome territory according to the models 3–5 (see section 2.1). Distances between each target and the nuclear center, as well as distances between the 'homologous' targets were calculated.

In each experiment distributions of distances for ten thousand up to one million configurations were computed on a SUN SuperSparc 10/40 workstation. The time needed for the calculation of such a distribution pattern took between 5 minutes and 5 hours depending on the number, geometrical shape and size of the territories.

2.3. Analytical calculations

The distribution of the centers of two spherical territories of the same size in a spherical nucleus (model 2) was calculated analytically. Considering the constraints mentioned above, the probability $P(\rho)$ for one of the two territories of radius r being located at a distance r to the center of a nucleus with radius R can be written as:

$$P(\rho) = \frac{\rho^2}{C} * \begin{cases} 4\{(R-r)^3 - (2r)^3\}, \\ \quad 0 \le \rho \le R - 3r \\ 4(R-r)^3 - (R - r - y(\rho) - \rho)^2 * \\ (2(R-r) + y(\rho) + \rho) \\ -(2r + y(\rho))^2(4r - y(\rho)), \\ \quad |R - 3r| \le \rho \le R - r \\ 0 \qquad R - r < \rho \end{cases}.$$

with C being a normalizing constant and $y(\rho)$ defined as

$$y(\rho) \overset{def}{=} \frac{1}{2\rho}\left(R^2 - 2Rr - 3r^2 - \rho^2\right).$$

Accordingly, the probability $\tilde{P}(\delta)$ of the two territories being a distance δ apart can be written as:

$$\tilde{P}(\delta) = \frac{1}{D} * \begin{cases} \delta^5 - 12(R-r)^2\delta^3 + 16(R-r)^3\delta^2, \\ \quad 2r \le \delta \le 2(R-r) \\ 0 \qquad \text{else} \end{cases}.$$

The normalizing constant D is given by

$$D = \frac{16}{3}\left(R^3 + 3Rr^2 - 2r^3\right)(R-2r)^3$$

3. Results

In this study we consider the effects of topological constraints on the distribution of chromosome territory mass centers (model 2) and subchromosomal targets (models 3–5; for details of model choice see section 2.1). Two constraints were studied in detail (a) the constraint of territory extension by the nuclear boundary, i.e. territories must not intersect the nuclear boundary and (b) the constraint of territory self-avoidance, i.e. territories occupy mutually exclusive nuclear subvolumes and thus must not intersect each other. Models 2–5 were compared with model 1, which considers the independent and uniform distribution of point-like targets without any topological constraints except for the nuclear boundary. The range of model territory sizes tested in model simulations exceeded the range expected for the territory size of the largest and smallest human chromosome, i.e. no. 1 and no. 21.

3.1. Topological constraints of chromosome territory distribution

3.1.1. Dependence on territory size Figure 2 shows the distribution of target–nuclear-center and target–target distances obtained for the centers of a pair of spherical territories in a spherical model nucleus (i.e. model 2). The curves in figure 2(a) indicate that the larger the territory size, the closer the centers of the territories are located

towards the center of the model nucleus. Figure 2(b) shows that the range of distances observed between two territory centers decreases with increasing territory size. Additionally, the curves in figure 2(a) and (b) show a cut off at the right side which reflects the fact that the center of a spherical territory cannot be closer to the nuclear boundary than the territory radius (constraint of territory extension). The cut off obtained on the left side of the curves shown in figure 2(b) is explained by the fact that the centers of two spherical territories cannot be closer to each other than the sum of their radii (constraint of territory self-avoidance).

The distribution of distances between territory centers and nuclear centers, as well as the distances between two 'homologous' territory centers were also calculated analytically for the case of a pair of spherical territories distributed within a spherical cell nucleus (model 2, see Models and Monte Carlo simulations). The analytically calculated distributions were identical with the simulated distributions within small statistical errors (< 0.1%), confirming the reliability of the Monte Carlo simulation results (data not shown).

3.1.2. Dependence on the number of territories To study how the arrangement of a pair of chromosome territories would be affected by a smaller second pair of chromosome territories, a second pair with a radius r_S varying from 0.0 (i.e. points) to r_L was added to the larger first pair having a fixed radius r_L. The distributions of the centers of the four territories (figure 1, model 2) were calculated for various combinations of territory sizes. Figure 3(a) and (b) shows the resulting mean territory center (TC)—nuclear center (NC) distances for the larger territory pair (TC_L–NC) depending on the size of the smaller pair (figure 3(a)) and vice versa the mean territory center—nuclear center distances of the smaller territory pair depending on the size of the larger pair (TC_S–NC, figure 3(b)). The mean chromosome center–nuclear center distance ($TC_{L,S}$–NC) for one pair of territories with fixed size increases with the size of the other pair of territories. In agreement with figure 2(a), figure 3(c) shows that TC_L–NC is always smaller than TC_S–NC, i.e. the centers of the larger territories in most model nuclei are located more peripherally than the centers of the smaller territories.

Figure 3(d) and (e) presents data for the distances between the centers of the two homologous territories. The second territory pair causes a slight increase in the mean distances between the centers of the first pair. In agreement with figure 2(b), a comparison of the mean distance between the centers of the two smaller territories (TC_S–TC_S) and the centers of the two larger territories (TC_L–TC_L) shows that the latter distance is generally smaller. For a few cases, however, figure 3(f) demonstrates that TC_L–TC_L exceeds TC_S-TC_S. This result reflects the fact that mean distances are influenced by both the territory self-avoidance and the territory extension/nuclear boundary constraint. In summary, the data presented in figure 3 demonstrate that the distribution of a single pair of chromosome territories in a model nucleus is only slightly affected by the additional consideration of a second pair.

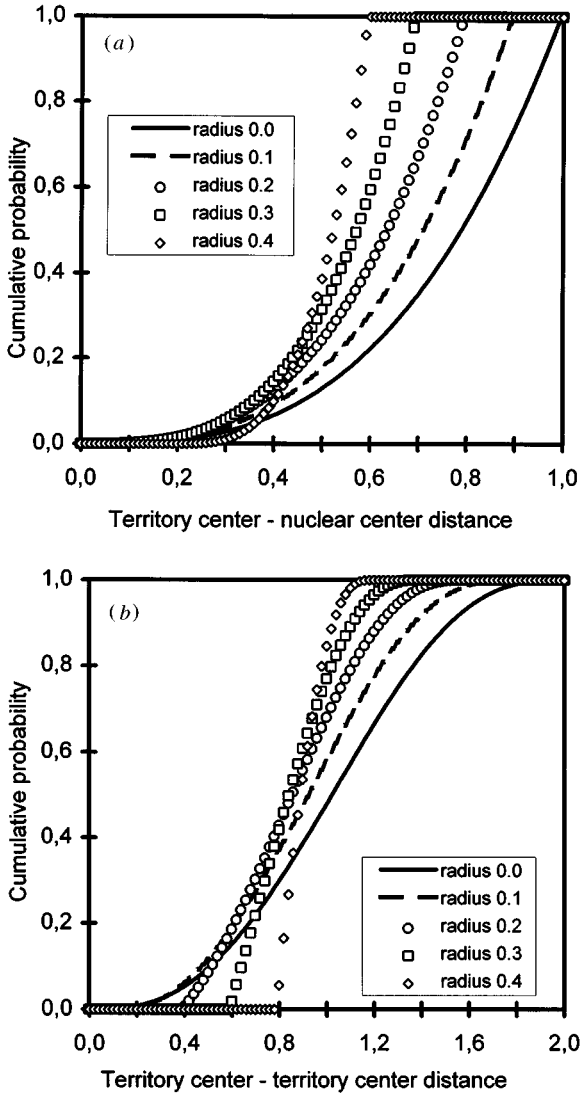

Figure 2. Cumulative frequency curves of distances obtained by three-dimensional Monte Carlo simulation experiments in spherical model nuclei containing a pair of spherical chromosome territories. Radius of the model nucleus is $r = 1$. (a) Distances between territory centers and the nuclear center. (b) Distances between the centers of the two territories. The radius of the chromosome territories was varied from 0 to 0.4, which is a little below the upper limit 0.5. Note that two territories with $r > 0.5$ do not fit into the model nucleus (constraints of self-avoidance and territory extension, for details see section 2.1).

3.1.3. Dependence on the shape of the model cell nucleus and model territory The shape of the model nucleus was varied to study the influence of the parameters

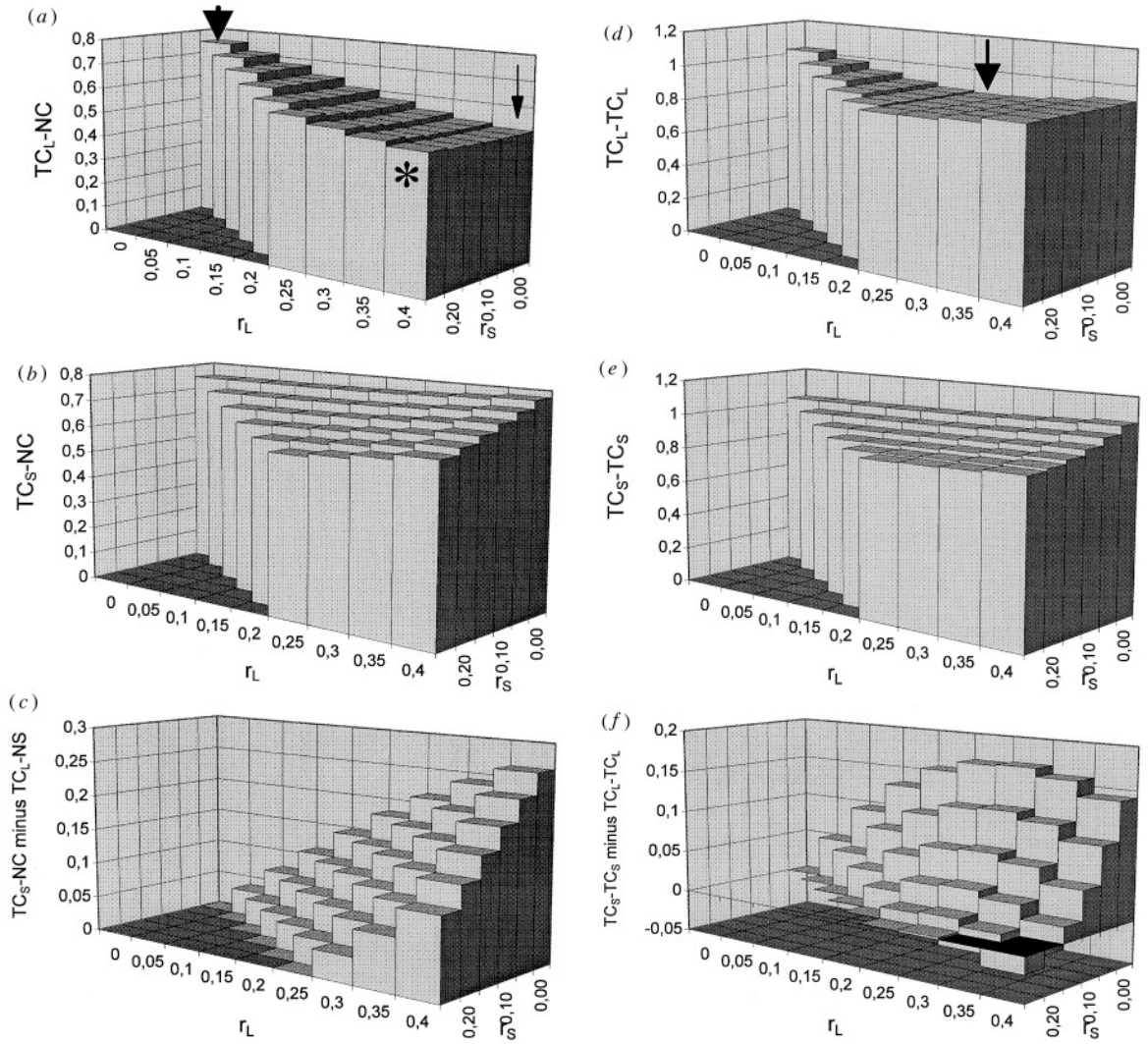

Figure 3. Influence of the presence of two pairs of territories on the mean territory center–nuclear center distances (a–c) and on the mean distances between the centers of 'homologous' territories (d–f) for 39 combinations of territory sizes. Two pairs of spherical territories with different radii r_L (larger territory) and r_S (smaller territory, $0.5 > r_L \geq r_S$) were distributed in a spherical model nucleus (radius $R = 1$) by Monte Carlo simulations; r_L was varied between 0 and 0.4, r_S between 0 and 0.25. Each column in (a), (b), (d) and (e) represents a mean distance (for definition see below) from 10^4 to 10^6 simulations. (a) The mean distance between the centers of the larger spherical territories (TC_L) and the center of the spherical model nucleus (NC) is represented by the height of each column. This distance (TC_L–NC) reaches its maximum 0.75, when r_L and r_S become zero (column depicted by thick arrow). With increasing r_L the mean distance TC_L–NC decreases. For example, TC_L–NC decreases from 0.75 to 0.51, when r_L increases from 0 (thick arrow) to 0.40 (thin arrow) and $r_S = 0$. The columns from back to front indicate that TC_L–NC is only slightly affected (less than 3%), when r_S increases. For example TC_L–NC increases from 0.51 to 0.52 when r_S increases from 0 to 0.25 and $r_L = 0.40$ (columns depicted by thin arrow and asterisk respectively). (b) Mean territory center–nuclear center distance for the smaller pair of territories TC_S–NC. This distance increases only slightly, when r_L increases from 0 to 0.40 . (c) Differences between TC_S–NC and TC_L–NC. (Column heights in (a) are subtracted from column heights in (b)). For all combinations of different territory sizes tested the difference is positive. This indicates that on average the centers of smaller territories are placed in a more peripheral position than centers of larger ones by topological constraints. In individual nuclei, however, the centers of smaller territories can be observed both more peripherally or more centrally as compared with the centers of the larger territories. (d) Mean distance between the centers of the two larger territories TC_L–TC_L. Note that the distance reaches the minimum at medium values of r_L (column depicted by arrow) while the size of r_S is nearly irrelevant. (e) Mean distance between the centers of the two smaller territories TC_S–TC_S. It increases only slightly, when r_L increases from 0 to 0.40. (f) Differences between TC_S–TC_S and TC_L–TC_L. (Column heights in (d) are subtracted from column heights in (e).) For all combinations of territory sizes tested the differences are smaller than 15%. For most combinations the difference is positive, indicating that on average the centers of the two smaller territories lie further apart from each other than the two larger ones. A small effect in the opposite direction (i. e. centers of larger territories lie slightly further apart) is observed for three of the combinations.

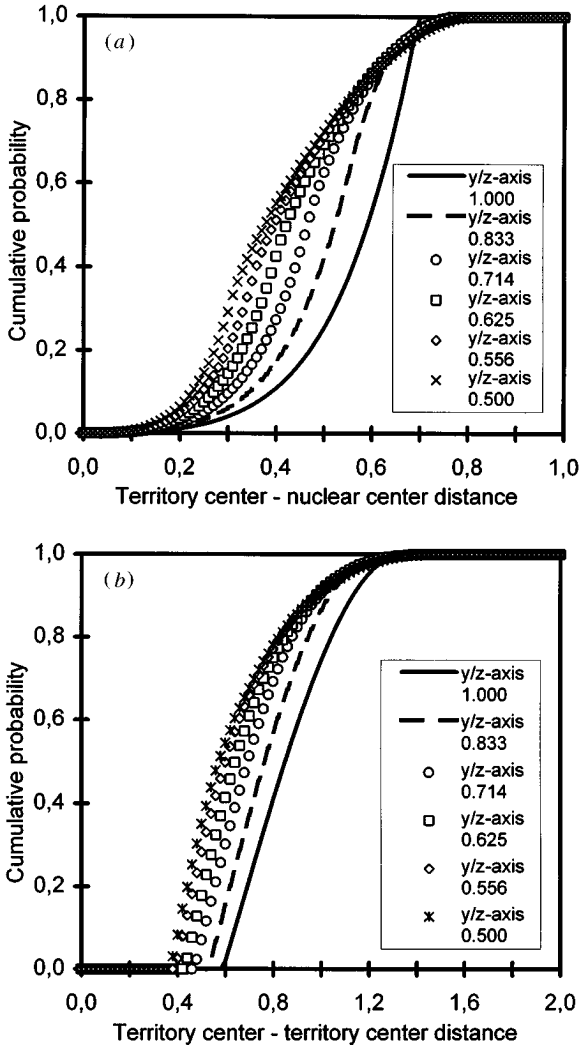

Figure 4. Influence of nuclear shape on territory distribution. (a) Distances between the centers of the larger territories and the nuclear center. (b) Distances between the centers of the two larger territories. Cumulative frequency curves were obtained by three-dimensional Monte Carlo simulation experiments. Model nuclei with various shapes contain two pairs of spherical chromosome territories (r_L = 0.30, r_S = 0.25). The shape of the nuclei was varied from a sphere ($R_{X,Y,S}$ = 1.0) to an ellipsoid (R_X = 1, $R_{Y,Z}$ = 0.5).

on the distribution of two pairs of territories. The cell nucleus was approximated by an ellipsoid with two smaller half axes $R_y = R_z$ and one larger half axis R_x normalized to 1.0 or by a sphere. The volume of the territories relative to the nuclear volume was the same for spherical and ellipsoidal nuclei.

Figure 4 shows the distribution of the two larger, spherical territories in dependence of the eccentricity of the cell nucleus. In these simulations the radius r_L (r_S) of the larger (smaller) territories was chosen to be 0.30 (0.25) of the radius of the spherical nucleus. The larger model territory comprises a fraction of 2.6% of the nuclear volume and therefore also 2.6% of the diploid human genome under the assumption of a uniform chromatin density. This approximately reflects the DNA content of the X chromosome (see section 3.2.1) and is in accordance with volume measurements of painted chromosome X-territories (Bischoff *et al* 1993), while the assumed size of the smaller territory correlates with the DNA content of a chromosome 14 (Morton 1991). The radii of the respective territories were determined as $r' = 3\sqrt{r^3 * R_{y,z}^2}$, since the volume ratio between the spherical and the ellipsoidal nucleus is $V_{\mathrm{ell}}/V_{\mathrm{sph}} = R_{y,z}^2$.

Figure 4(a) demonstrates that with increasing eccentricity of the cell nucleus the centers of the territories are located closer to the nuclear center. A similar tendency can be seen in figure 4(b) for the distances between two territory centers.

The influence of the chromosome territory shape on the distribution of the territory center was studied in a two-dimensional model experiment. In this experiment the territories were represented in a circular nucleus either by two circular territories (figure 5(a)) or by two ellipses of the same area with an axis ratio of 1:0.5 (figure 5(b)). The difference induced by the eccentricity of the territories is small, being mostly expressed for relatively large territories with a radius of 40% of the nuclear radius.

3.2. Topological constraints of subchromosomal target distributions

In addition to the distribution of the centers of entire chromosome territories (model 2) Monte Carlo simulations were performed to compute the distributions of points reflecting subchromosomal targets. Different target distributions were simulated according to models 3, 4 and 5 (compare figure 1 and Models and Monte Carlo simulations). In model 3 targets were distributed at random within chromosome territories. In models 4 and 5 the targets were located at chromosome territory surfaces either at random (model 4) or under the additional constraint of a specific territory orientation (model 5). The resulting distributions were compared with each other and with the distribution of point-like targets without geometrical constraints (model 1).

3.2.1. Dependence of target distributions on the choice of model Figure 6 shows the resulting target–nuclear center (figure 6(a,c,e,g)) and 'homologous' target–target (figure 6(b,d,f,h)) distributions for two pairs of chromosome territories representing the human chromosomes with the largest and smallest DNA content, i.e. chromosomes no. 1 and 21. As noted above the volumes of the territories were chosen under the simplified assumption that the 46 chromosome territories present in a human diploid cell nucleus completely fill the nuclear volume and that each

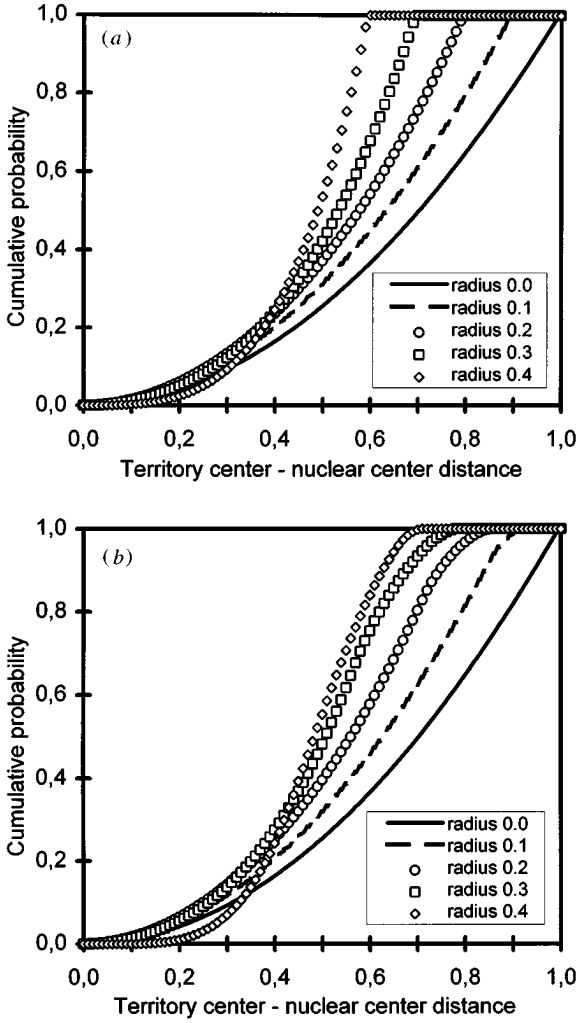

Figure 5. Influence of the territory shape on territory distribution. Cumulative frequency curves of territory center–nuclear center distances were obtained by two-dimensional Monte Carlo simulation experiments in circular model nuclei with radius $r = 1$. (a) Circular territories. (b) Elliptical territories, which occupy the same area as those in (a), whereas the ratio of the major and minor axis was 1:0.5.

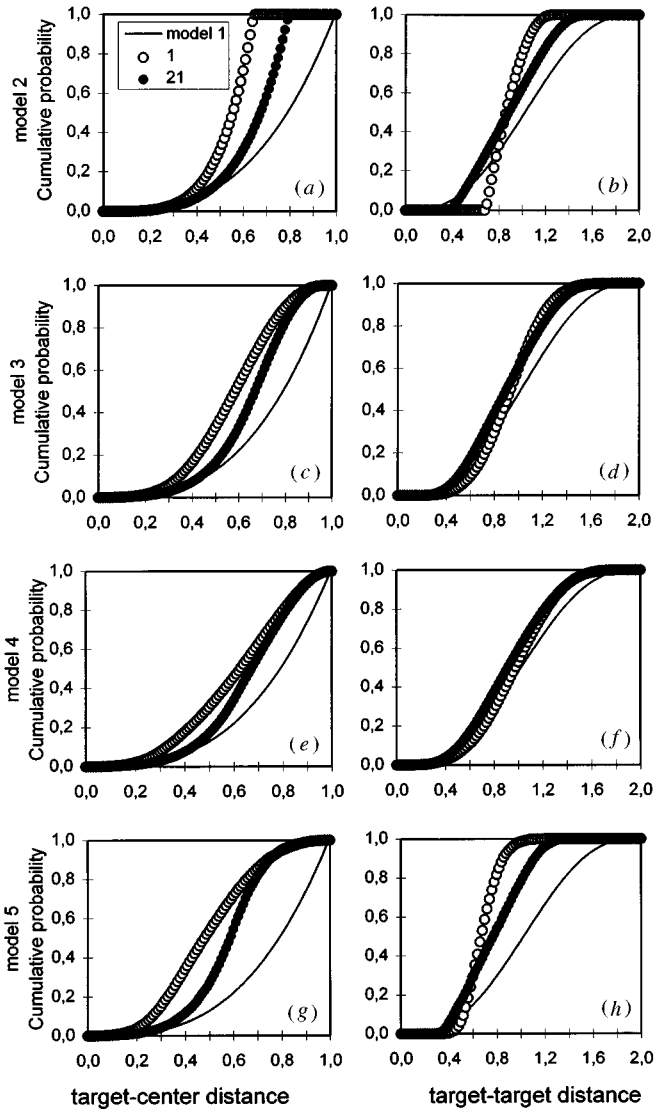

Figure 6. Three-dimensional target–nuclear center distances (a,c,e,g) and target–target distances (b,d,f,h) for targets belonging to territories which represent the largest and smallest human chromosomes, i.e. no. 1 (open circles) and no. 21 (filled circles) (for further details see section 3.2.1). Monte Carlo simulation experiments were performed for models 2 (a,b), 3 (c,d), 4 (e,f) and 5 (g,h). The cumulative frequency curve for model 1 (solid line) is shown in each graph for comparison.

individual territory occupies a fraction of the nuclear volume proportional to its DNA content (for DNA contents of human chromosomes see Morton 1991). Hence, we assume $r \approx 0.35$ for chromosome 1 and $r \approx 0.20$ for chromosome 21.

Figure 6 demonstrates that the cumulative probability curves are distinctly different, in particular for models 1, 2 and 5 and also depend on chromosome territory size. On the other hand, the distributions obtained for models 3 and 4 are rather similar, and it seems unlikely that they could be distinguished experimentally.

3.2.2. Comparison with experimental results In this section we compare the model distributions of targets as described above with three experimentally observed chromosome target distributions.

Figure 7(a) shows the target–nuclear center distribution obtained for the heterochromatic band 1q12 in PHA-stimulated and formaldehyde fixed lymphocyte nuclei (Dietzel *et al*, see accompanying paper). Following fluorescence *in situ* hybridization with the 1q12 specific DNA-probe pUC1.77 a three-dimensional evaluation was performed using axial light microscopic tomography (Bradl *et al* 1994). Obviously, the target–nuclear center

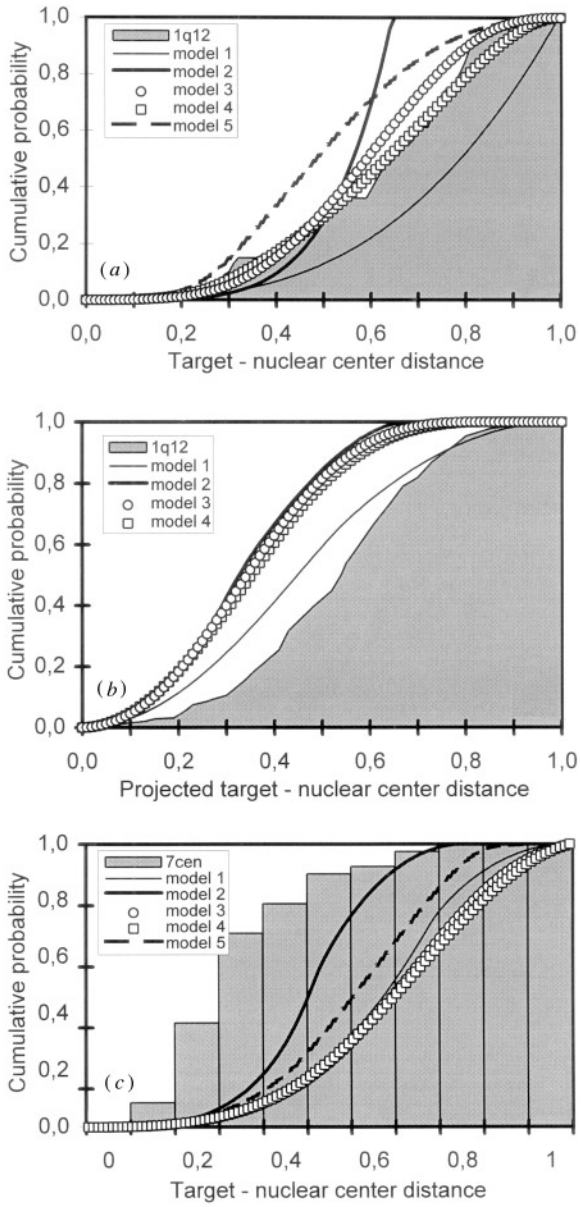

Figure 7. Comparison of target–nuclear center distance distributions derived by Monte Carlo simulations of model nuclei and by actual measurements of cell nuclei after fluorescence *in situ* hybridization. Model 1 (thin solid line), model 2 (thick solid line), model 3 (circles), model 4 (squares), model 5 (dashed line), compare figure 1. Radii of model territories were chosen according to the DNA content of the experimentally examined human chromosome ((a,b): #1 with visualization of band 1q12, (c): #7 with visualization of the centromeric heterochromatin in (c). It was assumed that each individual territory occupies a fraction of the entire nuclear volume proportional to its DNA content (for details see sections 2.2 and 3.2.1). (a) Three-dimensional target–nuclear center distances obtained for the heterochromatic band 1q12 in PHA-stimulated human lymphocyte nuclei (Dietzel *et al* see accompanying paper). Spherical model nuclei and territories with radius $r = 0.35$ were used. (b) Two-dimensional projections of 1q12–nuclear center distances obtained in human amniotic fluid cells (Volm 1992). Monte Carlo Simulations were performed for two-dimensional projections of three-dimensional distances in ellipsoid model nuclei. The radius of a spherical territory representing the DNA content of chromosome 1 is $r = 0.22$. This radius is smaller than the radius given in (a) for the same territory in a spherical model nucleus because the radii (half axes) of the model nuclei were chosen $R_x : R_y : R_z = 1 : 0.5 : 0.25$, which reflects the typical shape of an amniotic fluid cell nucleus. Accordingly the volume of the ellipsoid model nucleus is smaller than the volume of the spherical nucleus with $R = 1$, chosen in (a) and (c). (c) Three-dimensional target–nuclear center distances obtained for chromosome 7 centromeric heterochromatin in human fibroblast cell nuclei (Höfers *et al* 1993). The nuclei were modeled by ellipsoids with $R_x : R_y : R_z = 1.0 : 0.71 : 0.71$. The radius chosen for the spherical chromosome 7 model territories was $r = 0.24$.

distributions of models 3 and 4 fit the experimentally observed distribution of distances considerably better than the other model distributions did (including the frequently used model 1).

Figure 7(b) shows a two-dimensional projection of 1q12–nuclear center distances derived from human amniotic fluid cell nuclei after FISH with probe pUC1.77 (Volm 1992). In this projection the location of the target was recorded using a conventional epifluorescence microscope equipped with a camera lucida. The nuclear center of 250 nuclei with an apparently ellipsoidal shape was represented by the gravity center of the projected ellipse. The cumulative frequency curve of distances in this experiment is clearly not compatible with any of the model distributions. The difference between the experimental and model curves is more pronounced for models 2–4 than for the 'random point' model 1. Note that models 2–4 provide very similar distance distribution curves. This effect is due to the relatively flat shape of the amniotic fluid cell nuclei with a mean axis ratio of 1:0.5:0.25.

Figure 7(c) compares data published by Höfers *et al* (1993) with model distributions. These authors delineated the chromosome 7 centromeric heterochromatin (7(c)) in human fibroblast cell nuclei using FISH with a 7c specific probe. Laser confocal microscopy and image analysis procedures were applied to study the three-dimensional distribution of this target. The comparison of 7c–nuclear center distances with distances derived from models 2–5 and the 'random point' model 1 shows a highly significant difference in all cases ($p < 0.001$; one sided Kolmogorov Smirnov test).

4. Discussion

In previous studies chromosome target distributions in the cell nucleus have been compared with model distributions considering the uniform and independent distribution of point-like targets throughout the nuclear space (model 1). A highly significant deviation of chromosome target distributions from such a model distribution has often been found (Spaeter 1975, Rappold *et al* 1984, Emmerich *et al* 1989, Popp *et al* 1990, Höfers *et al* 1993). In case of sufficiently small, 'point-like' chromatin targets it has been expected that their random distribution in a cell nucleus would closely fit the random distribution of points in model nuclei of similar shape. This expectation was reasonable at a time when it was assumed that the chromatin fiber constituting an individual interphase chromosome should be distributed throughout the entire nuclear space (Comings 1968, Vogel and Schroeder 1974). However, such an assumption did not take into account the highly important geometrical constraints which result from the existence of chromosome territories (see Introduction). For such a case one should expect that the distribution of even a point-like subchromosomal target strongly depends on the topological constraints which affect the distribution of the respective chromosome territory. Hence, a comparison with model 1 is clearly not sufficient for a valid judgment of the random or non-random distribution of subchromosomal targets. In this investigation we studied the influence of two geometrical constraints, (i) the constraint of chromosome territory extension by the nuclear boundary, and (ii) the constraint of territory self-avoidance (see section 2.1).

It is our intention to develop and test improved models which take into account topological constraints of target distributions that result from the size and shape of chromosome territories and of the cell nucleus. In the present study, we have developed and tested four new models taking into account the distribution of the mass centers of the territories (model 2) and various possibilities for the localization of 'point-like' subchromosomal subregions. These targets were considered to be distributed randomly within the chromosome territory in model 3 and randomly at the surface of the chromosome territory in model 4. In model 5 we considered the possibility of a specific orientation of targets at the chromosome territory surface towards a centrosome attached to the nuclear envelope. As expected, model frequency distribution curves of three-dimensional target–nuclear center and target–target distances obtained by Monte Carlo simulations for models 2–5 deviated strongly from a uniform and independent distribution of points (model 1) and depended on territory size and shape, as well as on the nuclear shape. For a given territory size and shape the curves obtained for models 3 and 4 are relatively similar, while the curves for models 2 and 5 strongly differ. These results demonstrate that topological constraints in nuclei with a territorial chromosome organization must be considered even for point-like targets.

We expect that these models may be better suited to discriminate between 'random' distributions in the sense of a chromatin distribution resulting solely from constraints of chromosome territory/nuclear geometry and 'non-random' distributions, possibly established by additional mechanisms in a cell cycle and cell type specific way, e.g. by specific protein-DNA and protein-protein interactions. According to the first scenario the neighborhood of chromosome territories and chromosomal subregions, respectively, could be functionally meaningless. In contrast, the second scenario would imply a dynamic and functionally important suprachromosomal nuclear organization. Such 'non-random' target distributions should strongly deviate from the distributions which result solely from the geometrical constraints mentioned above. This view is supported by a number of studies which have indicated cell cycle and cell type specific chromosome arrangements (Weimer *et al* 1992, Ferguson and Ward 1992, for reviews see Manuelidis 1990, Lichter *et al* 1991, Haaf and Schmid 1991). The development of multicolor FISH, three-dimensional

fluorescence microscopy and quantitative image analysis procedures has made it possible to define subchromosomal target distributions experimentally and to compare them with model distribution curves.

Although models 2–5 are considerably advanced in comparison with model 1, they still should only be considered as a first approximation of the topological constraints which affect chromosomal arrangements in the cell nucleus. Nuclei and chromosome territories were modeled by spheres and ellipsoids, respectively. A distinct size and rigid structure was assumed for each chromosome territory, although even homologous territories can considerably vary in size and shape (Eils *et al* 1995b and our unpublished data). The assumption that the fraction of the nuclear volume occupied by a given chromosome territory is proportional to its DNA content has not been proven so far. We do not know to what extent the actual shape of a given territory is influenced by neighboring territories and/or other macromolecular nuclear domains (Spector 1993). Further, the possibility of dynamic changes of territory shape and positioning has to be considered (de Boni 1994). It is possible, even likely, that the nuclear volume occupied by all chromosome territories is considerably smaller than the entire nuclear volume. The remaining space between the chromosome territories may be filled by the nucleoli and other macromolecular nuclear domains (Zirbel *et al* 1993). In our present models we have neglected the presence of nucleoli and their effect on the positioning of chromosome territories. If nucleoli and chromosome territories bearing nucleolus organisator regions, i.e. human chromosomes 13, 14, 15, 21 and 22, are preferentially located in the central part of the nucleus, they should force other chromosome territories more towards the nuclear periphery. Considering the apparent complexity of a functional and dynamic nuclear architecture, detailed models of chromosome territory distribution under topological constraints require a high level of sophistication. However, given the present limitations of our knowledge of this architecture, we did not wish to make models unnecessarily complicated. Instead, it was our intention to demonstrate the importance of geometrical constraints and to point out some of their consequences.

It is interesting to note that the distribution of a given pair of chromosome territories was only slightly affected by the additional distribution of a second pair of territories. Such effects may become more pronounced, when all 46 chromosome territories of a human diploid cell nucleus are simultaneously modeled. For model 2, which describes the distribution of the center of mass for spherical chromosome territories, we noted that larger territories became distributed closer to the nuclear center than smaller ones, regardless of whether the model nucleus was simulated by a sphere or an ellipsoid. The same effect was observed in preliminary simulations where we have modeled nuclei with all 46 territories allowing for variations in shape (Eils *et al* 1995a, Münkel *et al* , unpublished model simulations).

As exemplified in the result section, a comparison of the model target distributions simulated in this study with experimentally observed chromosome target distributions indicates that model distributions in some cases fit reasonably well the observed target distributions, while in other cases measured target distributions deviate greatly from any of the model distributions studied so far. It would be clearly premature to conclude that an experimental target distribution, which deviates strongly from these model distributions, must be strongly influenced by other factors than topological constraints. Such a finding may simply indicate that the assumptions underlying our present models do not provide a valid description of the topological constraints affecting the chromatin distribution in a real cell nucleus.

A close fit of experimentally observed target distributions with distributions predicted by a given model does in no way prove that the topological constraints, which govern the model target distributions, were decisive factors which brought about the observed experimental distributions. Such a fit may be simply coincidental. For example, the distribution of chromosome 7 pericentromeric heterochromatin observed in human lymphocyte nuclei fits best with model 1 (Dietzel *et al*, see accompanying paper). However, it would be clearly invalid to suggest that the distribution of chromosome 7 centromeres was not affected by the topological constraints, which result from the size and shape of chromosome 7 territories. On the other hand a close fit between a model curve and an experimental curve may help to formulate hypotheses for further experimental tests. For example, model 4 showed the best fit with the distribution of chromosome 17 pericentromeric heterochromatin observed in human lymphocyte nuclei (Dietzel *et al*, see accompanying paper), suggesting the positioning of this target at the chromosome territory surface. Two-color FISH experiments and confocal laser scanning microscopy (Eils *et al* 1996) have supported this hypothesis for the centromeric or centromer near heterochromatin positioning of several chromosomes.

Acknowledgments

CM was supported by a stipend from the Landesgraduiertenförderung of the Land Baden-Württemberg (LGFG 9127.1). RE and JI received stipends from the Graduiertenkolleg ‘Modeling and Scientific Computing in Mathematics and Science’ at the Interdisciplinary Center of Scientific Computing (IWR) of the University of Heidelberg. The work of TC and CC was supported by grants from the Deutsche Forschungsgemeinschaft (Cr59/14-3 and Cr60/11-1).

References

Binder K and Heermann D W 1993 *Monte Carlo Simulation in Statistical Physics: An Introduction* 2nd edn (Heidelberg: Springer)

Bischoff A, Albers J, Kharboush I, Stelzer E, Cremer T and Cremer C 1993 Differences of size and shape of active and inactive X-chromosome domains in human amniotic fluid cell nuclei *J. Microsc. Res. Tech.* **25** 68–77

Bradl J, Hausmann M, Schneider B, Rinke B and Cremer C 1994 A versatile 2π-tilting device for fluorescence microscopy *J. Microsc.* **176** 211–21

Carter K C, Bowman D, Carrington W, Fogarty K, McNeil J A, Fay F S and Lawrence J B 1993 A three-dimensional view of precursor messenger RNA metabolism within the mammalian nucleus *Science* **259** 1330–5

Comings D E 1968 The rationale for an ordered arrangement of chromatin in the interphase nucleus *Am. J. Hum. Gen.* **20** 440–60

Cremer T, Cremer C, Baumann H, Luedtke E K, Sperling K and Zorn C 1982 Rabl's model of the interphase chromosome arrangement tested in Chinese hamster cells by premature chromosome condensation and laser-UV-microbeam experiments *Hum. Gen.* **76** 290–2

Cremer T, Kurz A, Zirbel R, Dietzel S, Rinke B, Schröck E, Speicher M R, Mathieu U, Jauch A, Emmerich P, Scherthan H, Ried T, Cremer C and Lichter P 1993 Role of chromosome territories in the functional compartmentalization of the cell nucleus *Cold Spring Harbor Symp. Quant. Biol.* **58** 777-92

De Boni U 1994 The interphase nucleus as a dynamic structure *Int. Rev. Cytol.* **150** 149–71

Dietzel S, Weilandt E, Eils R, Münkel C, Cremer C and Cremer T 1996 Three-dimensional distribution of centromeric or paracentromeric heterochromatin of chromosomes 1,7,15 and 17 in human lymphocyte nuclei studied with light microscopic axial tomography *Bioimaging* **3** 121–33

Eils R, Saracoglu K, Münkel C, Imhoff J, Sätzler K, Bertin E, Dietzel S, Schröck E, Ried T, Cremer T and Cremer C 1995a Three-dimensional imaging approaches and Monte Carlo simulations: development of tools to study the morphology and distribution of chromosome territories and subchromosomal targets in human cell nuclei *Zoological Studies* **34** Supplement I 7–10

Eils R, Bertin E, Saracoglu K, Rinke B, Schröck E, Parazza F, Usson Y, Robert-Nicoud M, Stelzer E H K, Chassery J M, Cremer T and Cremer C 1995b Application of laser confocal microscopy and 3-D-Voronoi diagrams for volume and surface estimates of interphase chromosomes *J. Microsc.* **177** 150–61

Eils R, Dietzel S, Bertin E, Granzow M, Schröck E, Speicher M R, Volm T, Ried T, Robert-Nicoud M, Cremer C and Cremer T 1996 Three-dimensional reconstruction of painted human interphase chromosomes: active and inactive X-chromosome territories have similar volumes but differ in surface and shape, submitted

Emmerich P, Loos P, Jauch A, Hopman A H N, Wiegant J, Higgins M J, White B N, Van der Ploeg M, Cremer C and Cremer T 1989 Double *in situ* hybridization in combination with digital image analysis: A new approach to study interphase chromosome topology *Exp. Cell Res.* **181** 126–40

Ferguson M and Ward DC 1992 Cell cycle dependent chromosomal movement in pre-mitotic human T-lymphocyte nuclei *Chromosoma* **101** 557-65

Geiger B, Komitowski D, Jauch A, Hausmann M and Cremer C 1991 Optical sectioning and 3-D-image reconstruction to determine the volumes of specific chromosome regions in human interphase cell nuclei *Optik* **86** 113-9

Heslop-Harrison J S and Bennet M D 1990 Nuclear architecture in plants *Trends Gen.* **6** 401–5

Haaf T and Schmid M 1991 Chromosome topology in mammalian interphase nuclei *Exp. Cell Res.* **192** 325-32

Hahnfeldt P, Hearst J E, Brenner D J, Sachs R K and Hlatky L R 1993 Polymer models for interphase chromosomes *Proc. Natl. Acad. Sci.* **90** 7854–8

Höfers C, Jovin T M, Hummer G and Arndt-Jovin D J 1993 The localization of chromosome domains in human interphase nuclei. Three-dimensional distance determinations of fluorescence in situ hybridization signals from confocal laser scanning microscopy *Bioimaging* **1** 96–106

Kalos M H and Whitlock P A 1986 *Monte Carlo Methods* vol 1 (New York: Wiley)

Klar A, Aichelin J and Krüger J 1984 Model for the distribution of distance of specific chromosome regions in interphase nuclei *Hum. Gen.* **67** 322–5

Lichter P, Cremer T, Borden J, Manuelidis L and Ward D C 1988 Delineation of individual human chromosomes in metaphase and interphase cells by in situ suppression hybridization using recombinant DNA libraries *Hum. Gen.* **80** 224-34

Lichter P, Boyle A L, Cremer T and Ward D C 1991 Analysis of genes and chromosomes by non-isotopic in situ hybridization *Gen. Anal. Tech. Appl.* **8** 24–35

Manuelidis L 1985 Individual interphase chromosome domains revealed by in situ hybridization *Hum. Gen.* **71** 288–93

Manuelidis L and Borden J 1988 Reproducible compartmentalization of individual chromosome domains in human CNS cells revealed by in situ hybridization and three- dimensional reconstruction *Chromosoma* **96** 397–410

Manuelidis L 1990 A view of interphase chromosomes *Science* **250** 1533–40

Morton N E 1991 Parameters of the human genome *Proc. Natl. Acad. Sci. USA* **88** 7474–6

Pinkel D, Landegent J, Collins C, Fuscoe J, Segraves R, Lucas J and Gray J W 1988 Fluorescence in situ hybridization with human chromosome-specific libraries: Detection of trisomy 21 and translocations of chromosome 4 *Proc. Natl. Acad. Sci.* **85** 9138–42

Popp S, Scholl H P, Loos P, Jauch A, Stelzer E, Cremer C and Cremer T 1990 Distribution of chromosome 18 and X centric heterochromatin in the interphase nucleus of cultured human cells *Exp. Cell Res.* **189** 1–12

Rabl C 1885 Über Zelltheilung *Morphologisches Jahrbuch* (Leipzig) **10** 214–330

Rappold G A, Cremer T, Hager H D, Davies K E, Müller C R and Yang T 1984 Sex chromosome positions in human interphase nuclei as studied by in situ hybridization with chromosome specific DNA probes *Hum. Gen.* **67** 317–25

Sachs R K, van den Engh G, Trask B, Yokota H and Hearst J E 1995 A random-walk/giant-loop model for interphase chromosomes *Proc. Natl. Acad. Sci.* **92** 2710–4

Schardin M, Cremer T, Hager H D and Lang M 1985 Specific staining of human chromosomes in Chinese hamster/man hybrid cell lines demonstrates interphase chromosome territories *Hum. Gen.* **71** 281–7

Später M 1975 Nichtzufällige verteilung homologer chromosomen (Nr. 9 und YY) in interphasekernen menschlicher fibroblasten *Hum. Gen.* **27** 111–8

Spector D L 1993 Macromolecular domains within the cell nucleus *Ann. Rev. Cell Biol.* **9** 265–315

Van Dekken H, Pinkel D, Mullikin J, Trask B, van den Engh G and Gray J 1989 Three-dimensional analysis of the

organization of human chromosome domains in human-hamster hybrid interphase nuclei *J. Cell Sci.* **94** 299–306

Vogel F and Schroeder T M 1974 The internal order of the interphase nucleus *Humangenetik* **25** 265–97

Volm T 1992 Gibt es eine größenabhängige verteilung von chromosomen in menschlichen kultivierten fruchtwasserzellen? Untersuchungen mittels Fluoreszenz in situ hybridisierung chromosomenspezifischer DNA-Sonden mit digitaler bildanalyse *MD Thesis* Institute of Human Genetics and Anthropology, University of Heidelberg

Weimer R, Haaf T, Poot M and Schmid M 1992 Characterization of centromere arrangements and test for random distribution in G0, G1, S, G2, G1′ and early S′ phase in human lymphocytes *Hum. Gen.* **88** 673–82

Zirbel R M, Mathieu U R, Kurz A, Cremer T and Lichter P 1993 Evidence for a nuclear compartment of transcription and splicing located at chromosome domain boundaries *Chromosome Res.* **1** 93–106